Delineating associations of progressive pleuroparenchymal fibroelastosis in patients with pulmonary fibrosis

Eyjolfur Gudmundsson [1], An Zhao[1], Nesrin Mogulkoc[2], Frouke van Beek[3], Tinne Goos [4,5], Christopher J. Brereton[6], Marcel Veltkamp[3,7], Robert Chapman [8], Hendrik W. van Es[9], Helen Garthwaite[10], Bahareh Gholipour[11], Melissa Heightman[8], Arjun Nair [11], Katarina Pontoppidan[6], Recep Savas [12], Asia Ahmed[11], Marie Vermant[4,5], Omer Unat[2], Alex Procter[11], Laurens De Sadeleer [5], Emma Denneny [8], Timothy Wallis[6], Mark Duncan[11], Magali Taylor[11], Stijn Verleden[4,13], Sam M. Janes [14], Daniel C. Alexander[1], Athol U. Wells[15], Joanna Porter [8], Mark G. Jones [6], Iain Stewart [16], Coline H.M. van Moorsel[3], Wim Wuyts [4,5] and Joseph Jacob [1,14]

[1]Centre for Medical Image Computing, Department of Computer Science, UCL, London, UK. [2]Department of Respiratory Medicine, Ege University Hospital, Izmir, Turkey. [3]Interstitial Lung Diseases Center of Excellence, Department of Pulmonology, St Antonius Hospital, Nieuwegein, The Netherlands. [4]BREATHE, Department of Chronic Diseases and Metabolism, KU Leuven, Leuven, Belgium. [5]Department of Respiratory Diseases, University Hospitals Leuven, Leuven, Belgium. [6]NIHR Southampton Biomedical Research Centre and Clinical and Experimental Sciences, University of Southampton, Southampton, UK. [7]Division of Heart and Lungs, University Medical Center, Utrecht, The Netherlands. [8]Interstitial Lung Disease Service, Department of Respiratory Medicine, University College London Hospitals NHS Foundation Trust, London, UK. [9]Department of Radiology, St Antonius Hospital, Nieuwegein, The Netherlands. [10]Royal Free University Hospital NHS Foundation Trust, London, UK. [11]Department of Radiology, University College London Hospitals NHS Foundation Trust, London, UK. [12]Department of Radiology, Ege University Hospital, Izmir, Turkey. [13]Department of Respiratory Medicine, University of Antwerp, Antwerp, Belgium. [14]Lungs for Living Research Centre, UCL, London, UK. [15]Interstitial Lung Disease Unit, Royal Brompton Hospital, Imperial College, London, UK. [16]National Heart and Lung Institute, Imperial College London, London, UK.

Corresponding author: Joseph Jacob (j.jacob@ucl.ac.uk)

Shareable abstract (@ERSpublications)
Computerised pleuroparenchymal fibroelastosis (PPFE) progression was found to associate with mortality in idiopathic pulmonary fibrosis and fibrotic hypersensitivity pneumonitis but PPFE did not correlate strongly with measures of fibrosis progression https://bit.ly/3FKYQn7

Cite this article as: Gudmundsson E, Zhao A, Mogulkoc N, *et al*. Delineating associations of progressive pleuroparenchymal fibroelastosis in patients with pulmonary fibrosis. *ERJ Open Res* 2023; 9: 00637-2022 [DOI: 10.1183/23120541.00637-2022].

Received: 21 Nov 2022
Accepted: 1 Dec 2022

Abstract

Background Computer quantification of baseline computed tomography (CT) radiological pleuroparenchymal fibroelastosis (PPFE) associates with mortality in idiopathic pulmonary fibrosis (IPF). We examined mortality associations of longitudinal change in computer-quantified PPFE-like lesions in IPF and fibrotic hypersensitivity pneumonitis (FHP).

Methods Two CT scans 6–36 months apart were retrospectively examined in one IPF (n=414) and one FHP population (n=98). Annualised change in computerised upper-zone pleural surface area comprising radiological PPFE-like lesions (Δ-PPFE) was calculated. Δ-PPFE >1.25% defined progressive PPFE above scan noise. Mixed-effects models evaluated Δ-PPFE against change in visual CT interstitial lung disease (ILD) extent and annualised forced vital capacity (FVC) decline. Multivariable models were adjusted for age, sex, smoking history, baseline emphysema presence, antifibrotic use and diffusion capacity of the lung for carbon monoxide. Mortality analyses further adjusted for baseline presence of clinically important PPFE-like lesions and ILD change.

Results Δ-PPFE associated weakly with ILD and FVC change. 22–26% of IPF and FHP cohorts demonstrated progressive PPFE-like lesions which independently associated with mortality in the IPF cohort (hazard ratio 1.25, 95% CI 1.16–1.34, p<0.0001) and the FHP cohort (hazard ratio 1.16, 95% CI 1.00–1.35, p=0.045).

Interpretation Progression of PPFE-like lesions independently associates with mortality in IPF and FHP but does not associate strongly with measures of fibrosis progression.

Introduction

Idiopathic pulmonary fibrosis (IPF) is a progressive lung disease characterised by lower zone predominant honeycomb cysts and traction bronchiectasis [1] on computed tomography (CT) imaging [2]. IPF can show a variable disease course [3]. Quantifying disease progression on imaging is important and has primarily involved visual semi-quantification of changes in CT extents of honeycomb cysts, reticulation, ground glass opacities and traction bronchiectasis [4], patterns reflecting pulmonary sequelae of fibrotic damage. Yet estimation of serial CT change in these patterns have shown limited correlations with measures of disease progression [5–7] (change in forced vital capacity (FVC)) and variable correlation with mortality in IPF patients [7].

Computational analysis of CT imaging can identify alternative CT patterns such as vessel-related structures [8–10] which associate with mortality in patients with IPF. Exploration of novel imaging features has also delineated patterns such as pleuroparenchymal fibroelastosis (PPFE) which do not directly result from the fibrotic process, but which may influence patient survival [11]. PPFE is characterised by dense triangular pleurally based opacities occurring in the upper lobes on CT [12]. PPFE scored visually on a single baseline CT has been shown to associate with reduced survival time in IPF patients [11, 13] and other fibrosing lung diseases [14, 15]. Computer quantitation of baseline upper lobe PPFE-like lesions (incidence 25–36%) was shown to associate with mortality in IPF independent of baseline disease severity (measured by either FVC, CT interstitial lung disease (ILD) extent or diffusion capacity of the lung for carbon monoxide (D_{LCO})) and identified more patients with a poor outcome than equivalent semi-quantitative visual CT analysis [11]. PPFE-like lesions scored by computer did not associate with baseline measures of IPF-related fibrosis on univariable or multivariable analyses, suggesting that PPFE-related damage might represent injury occurring independent to IPF-related lung fibrosis [11].

Careful delineation of patients with clinically meaningful progressive PPFE-like lesions using computational analysis of time-series CTs may highlight a lung fibrosis endotype benefiting from alternative management strategies [16]. Sensitive quantification of progressive PPFE could also evaluate treatment response in future trials of therapies targeting PPFE and/or progressive fibrotic phenotypes [17] where PPFE change might influence outcome measures. Our current study therefore aimed to delineate in IPF and fibrotic hypersensitivity pneumonitis (FHP) populations the prevalence and prognostic impact of progressive PPFE-like lesions. We also examined whether PPFE change associated with other measures of disease progression in IPF.

Material and methods

Study subjects and clinical information

Patients with a multidisciplinary team diagnosis of IPF or FHP with two volumetric CT examinations separated by 6–36 months were identified from five medical centres (Ege University Hospital, Izmir, Turkey; St Antonius Hospital, Nieuwegein, the Netherlands; University Hospital Southampton NHS Foundation Trust, UK; University College London Hospitals NHS Foundation Trust, UK; University Hospitals Leuven, Belgium) (supplementary table S1). CONSORT diagrams for the two study populations are shown in figure 1 and supplementary figure S1; patient demographics for patients included in the study are shown in table 1. Approval for this retrospective study of clinically indicated pulmonary function and CT data was obtained from the local research ethics committees and Leeds East Research Ethics Committee: 20/YH/0120.

Visual CT evaluation

A subspecialist radiologist (J. Jacob) with 14 years of thoracic imaging experience determined lobar percentages of ILD (sum of ground glass density, reticulation, traction bronchiectasis volume and honeycomb cysts, averaged across six lobes [11]) on two timepoint CTs, and emphysema presence (absent/present) on baseline CTs of all IPF and FHP patients. Change in CT ILD extent was annualised ("Δ-ILD"). The radiologist was blinded to outcome data when visually evaluating the CTs of the study.

Computer-based CT evaluation

Computerised quantification of the percentage of visceral pleural surface (most peripheral 3 lung surface pixels) affected by radiological PPFE-like lesions was obtained on CT pairs of IPF and FHP patients as previously described [11]. PPFE-like lesions were only quantified in the upper zones (region extending from carina to 5 mm below lung apices – thereby avoiding capturing an apical cap) which approximated the upper lobes, where radiological PPFE is most typically found. A 2.5% threshold of PPFE extent on baseline imaging, derived in a previous IPF study [11], delineated clinically important PPFE at baseline for IPF and FHP cohorts.

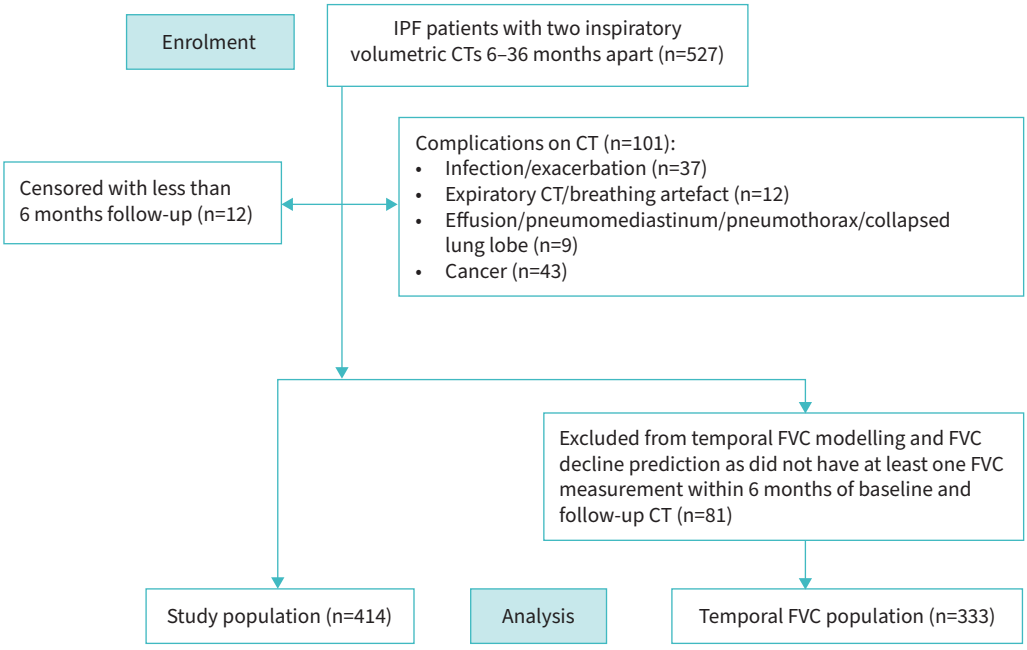

FIGURE 1 CONSORT diagram showing exclusions for IPF patients in the study. IPF: idiopathic pulmonary fibrosis; CT: computed tomography; FVC: forced vital capacity.

The annualised change in computerised upper-zone extent of PPFE-like lesions between scans ("Δ-PPFE") was calculated as the difference in computerised PPFE between the baseline and follow-up CTs, divided by the scan interval in years. It is important to account for the contribution of noise to the estimation of

TABLE 1 Patient demographics, pulmonary function indices and visual and computer-based scores of ILD and PPFE severity for IPF and FHP patients in the study

Variable	IPF cohort	FHP cohort	p-value
Patients n	414	98	
Baseline age years, median (range)	69 (32–95)	64 (28–85)	0.0001
Male/female %	24.2/75.8	62.2/37.8	<0.0001
Survival (alive/dead) %	44.4/55.6	54.1/45.9	0.11
Follow-up years, median (range)	2.2 (0.0–9.0)	2.7 (0.0–12.0)	0.013
Time between CT scans years, median (range)	1.1 (0.5–3.0)	1.1 (0.5–2.9)	0.81
Never-/ever-smokers %	30.7/69.3	50.0/50.0	0.0005
Antifibrotic (never/ever) %	30.7/69.3		
Baseline FVC % predicted	81.3±19.7	64.2±19.6	<0.0001
Baseline D_{LCO} % predicted	48.8±15.9	50.5±16.8	0.44
Baseline emphysema (absent/present) %	32.4/67.6	69.4/30.6	<0.0001
Baseline ILD extent %	39.0±12.3	33.3±14.0	0.0003
Δ-ILD %/year	7.7±8.7	4.0±5.6	<0.0001
Baseline PPFE extent %	2.0±2.4	1.9±2.3	0.74
Δ-PPFE %/year	0.8±2.0	0.8±2.4	0.93
Clinically important baseline PPFE prevalence %	29.5	26.5	0.65
Progressive PPFE prevalence %	21.5	25.5	0.47
Δ-PPFE-adj in progressive PPFE patients %/year	2.3±2.7	2.4±3.3	0.86

Pulmonary function indices, ILD extent and PPFE scores are described as mean±SD. Clinically important PPFE at baseline was defined as baseline PPFE extent >2.5%. Progressive PPFE was defined as Δ-PPFE >1.25%/year. ILD: interstitial lung disease; PPFE: pleuroparenchymal fibroelastosis; IPF: idiopathic pulmonary fibrosis; FHP: fibrotic hypersensitivity pneumonitis; CT: computed tomography; FVC: forced vital capacity; D_{LCO}: diffusing capacity of the lung for carbon monoxide; Δ-ILD: annualised change in ILD extent between CT scans; Δ-PPFE: annualised change in computerised upper-zone PPFE between scans; Δ-PPFE-adj: Δ-PPFE above scan noise.

PPFE change between CT scans. Noise can occur between CT timepoints due to differences (for example) in CT acquisition parameters including scanner model and reconstruction algorithm variability, in the level of patient inspiration, and in patient positioning. Δ-PPFE of 1.25% or more of the pleural surface area was used to identify patients with morphologically definitive "progressive" radiological PPFE-like lesions. The estimation of noise contained within the longitudinal CT imaging was determined by calculating one half of the standard deviation of baseline PPFE in the derivation IPF cohort [11], which corresponds to a moderate effect size. This method has previously been suggested to determine the minimal clinically important difference in biomarker studies in IPF [18–20]. A continuous variable ("Δ-PPFE-adj") reflecting definitive change in extent of PPFE-like lesions above scan noise was created by subtracting 1.25% from Δ-PPFE values of progressive radiological PPFE patients and setting Δ-PPFE-adj values to 0% for non-progressive patients.

Modelling strategy

Linear mixed-effects (LME) regression analyses, with a single fixed effect and a random intercept for each centre, investigated the association between longitudinal change of ILD extent and PPFE extent, and baseline ILD, PPFE, D_{LCO} % predicted, and FVC % predicted in both cohorts. LME models with multiple fixed effects were also used to investigate the association between change in FVC and Δ-PPFE. The temporal trajectories of FVC measurements were modelled between baseline and follow-up CTs separately for each cohort, with a random intercept for each centre and each subject, and with a random slope for each subject. These models included fixed effects of age at baseline, patient sex, smoking status (never/ever), baseline emphysema presence, baseline FVC % predicted, study time and Δ-PPFE. In the IPF cohort, these models also included fixed effects of antifibrotic use across follow-up (never/ever).

Across all LME models for FVC, patients who did not have at least two absolute FVC measurements (one within 6 months of baseline CT and another within 6 months of follow-up CT) were excluded (IPF: 81 excluded out of 414; FHP: 20 excluded out of 98). Modelled FVC measurements were restricted to 6 months prior to the baseline CT of each patient and 6 months after the follow-up CT of each patient, to ensure that FVC trajectories were representative of the development of disease between the scans.

Univariable and multivariable Cox regression analyses explored determinants of mortality, with a single frailty variable for centre to adjust for mean differences between patient centres within each cohort. Entry time for survival analysis was taken as the date of second CT. All multivariable mortality models were adjusted for patient age at baseline, patient sex, smoking status (never/ever), baseline emphysema presence (absent/present), Δ-ILD, clinically important PPFE at baseline (no/yes) and D_{LCO} % predicted. Antifibrotic use (never/ever) adjustments were used in the IPF cohort only.

Baseline D_{LCO} % predicted and baseline FVC % predicted were considered if available within 3 months of baseline CT. Missing baseline D_{LCO} % predicted and baseline FVC % predicted were imputed and considered missing at random (details in online supplementary material).

Statistical analysis

Data are presented as patient proportions (%) or mean±SD or medians (with range of values), as appropriate. Differences in categorical variables were assessed using the Chi-squared test. Differences in medians of continuous variables were assessed using the two-sided Mann–Whitney U-test. Differences in means of continuous variables were assessed using the two-sided t-test. In three-group comparisons, a Kruskal–Wallis rank sum test evaluated differences in medians and a one-way ANOVA evaluated differences in means. A p-value <0.05 was considered significant across all analyses. Multivariable linear models were tested for heteroscedasticity using the studentised Breusch–Pagan test [21]. The Concordance index (C-index) compared the goodness of fit of Cox regression models [22]. R^2 values reported for LME models are the "marginal" R^2, which describes the proportion of variance explained by fixed factor(s) alone [23]. Bootstrapping with 500 iterations was used to estimate sampling distributions of the C-index. Kaplan–Meier curves were truncated at 5 years. LME model analyses, Cox regression and Kaplan–Meier analyses, and multiple imputations were performed with the lme4, survival and mice packages in R, respectively (version 4.1.1 with RStudio version 1.4.1717; RStudio, Boston, MA, USA).

Results

Baseline data

Demographic data, baseline pulmonary function tests, and mean visual ILD extent and computerised PPFE scores for the IPF cohort (n=414) and the FHP cohort (n=98) are shown in table 1. Baseline characteristics of IPF patients and FHP patients excluded from the study are shown in supplementary tables S2 and S3, respectively.

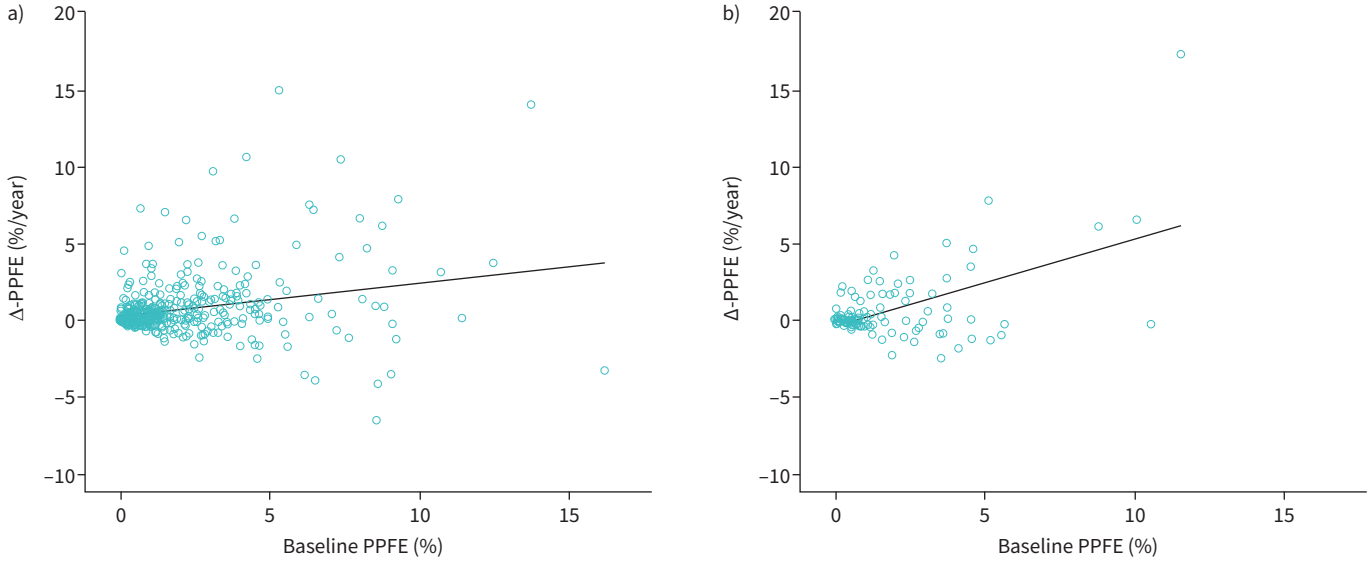

FIGURE 2 Association between Δ-PPFE and baseline PPFE extent in a) the IPF cohort (effect: 0.21%/year, 95% CI 0.13–0.29%/year, p<0.0001, R^2=0.06) and b) the FHP cohort (effect: 0.56%/year, 95% CI 0.38–0.75%/year, p<0.0001, R^2=0.28). PPFE: pleuroparenchymal fibroelastosis; Δ-PPFE: annualised change in computerised upper-zone PPFE between scans; IPF: idiopathic pulmonary fibrosis; FHP: fibrotic hypersensitivity pneumonitis.

Computerised PPFE extent associations

The prevalence of clinically important PPFE (*i.e.*, PPFE extent >2.5%) on baseline imaging was 29.5% in the IPF cohort and 26.5% in the FHP cohort (table 1). Baseline computerised PPFE extent weakly associated with Δ-PPFE in the IPF cohort but slightly more strongly in the FHP cohort (figure 2 and supplementary table S4). Baseline PPFE weakly associated with Δ-ILD in univariable models in the IPF cohort only (supplementary figure S2 and table S4).

Δ-PPFE weakly associated with Δ-ILD in the IPF cohort but not the FHP cohort (supplementary figure S3 and table S4). Δ-PPFE weakly associated with baseline D_{LCO} % and baseline FVC % in multivariable models in both cohorts (supplementary tables S4 and S5 and figures S4 and S5). Comparisons between baseline ILD and Δ-ILD and Δ-PPFE are shown in supplementary figures S6 and S7.

PPFE change and FVC decline

Demographic data, baseline pulmonary function tests, and mean visual ILD extent and computerised PPFE scores for patients included and excluded from FVC modelling in the IPF cohort and the FHP cohort are shown in supplementary tables S6 and S7, respectively. Δ-PPFE weakly associated with FVC change in univariable models in the IPF cohort only (−0.13 L·year^{-1}, 95% CI −0.18– −0.08 L·year^{-1}, p<0.0001, R^2=0.07) and in multivariable models in the IPF cohort only (effect: −0.09 L·year^{-1}, 95% CI −0.13– −0.05 L·year^{-1}, p<0.0001, R^2=0.34) (supplementary tables S8 and S9). Results were maintained in non-imputed models in both cohorts (supplementary table S10).

PPFE change associations with mortality

In univariable Cox regression models in the IPF cohort, covariates significantly associated with mortality included: baseline D_{LCO} % predicted, baseline FVC % predicted, baseline ILD extent, baseline PPFE extent, presence of clinically important PPFE at baseline, Δ-PPFE and Δ-PPFE-adj (supplementary table S11). In the FHP cohort, covariates significantly associated with mortality in univariable Cox regression models included: patient age at baseline, baseline D_{LCO} % predicted, baseline ILD extent, baseline PPFE extent, Δ-PPFE and Δ-PPFE-adj (supplementary table S11).

In multivariable Cox regression models, Δ-PPFE was significantly associated with mortality in the IPF cohort (hazard ratio (HR) 1.20, 95% CI 1.13–1.28, p<0.0001) and the FHP cohort (HR 1.18, 95% CI 1.05–1.34, p=0.008) (supplementary table S12). Results were maintained in non-imputed models in both cohorts (supplementary table S13). Multivariable Cox regression models without adjustment for Δ-PPFE are shown in supplementary table S14.

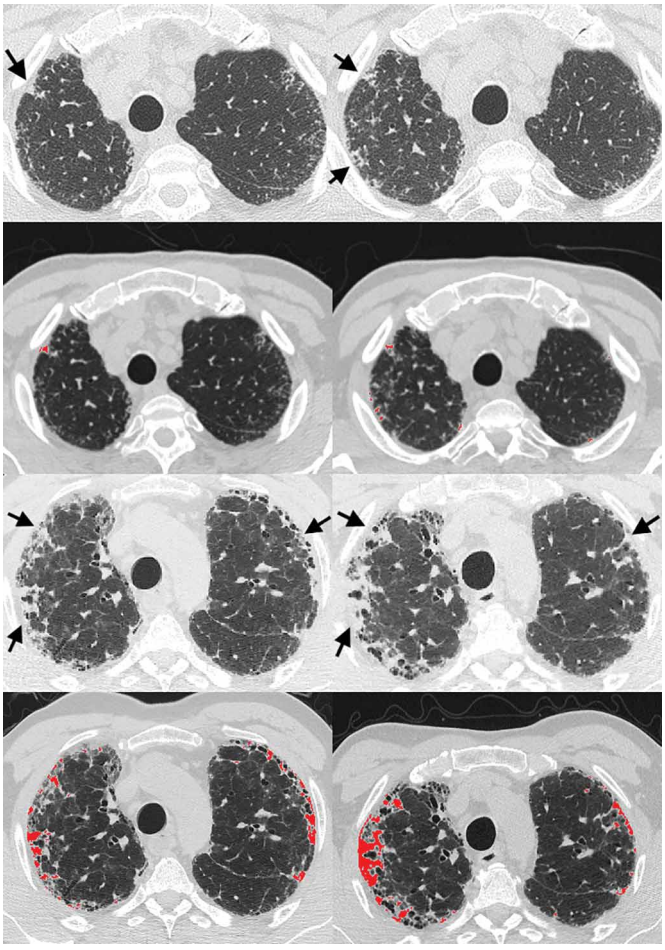

FIGURE 3 Visual characteristics of progressive pleuroparenchymal fibroelastosis (PPFE). Baseline (left column) and follow-up (right column) computed tomography (CT) scans in patients diagnosed with idiopathic pulmonary fibrosis by multidisciplinary team. The top two rows show axial CT images of the upper zones taken 13 months apart in a 73-year-old male with normal baseline forced vital capacity (FVC) (83%) and diffusion capacity of the lung for carbon monoxide (D_{LCO}) (74%). Arrows (top row) show areas of PPFE increasing in extent on the second CT, also highlighted by image overlays of PPFE regions (second row). The bottom two rows show axial CT images taken 9 months apart in a 54-year-old male with abnormal baseline FVC (46%) and D_{LCO} (35%). Arrows (third row) show more extensive PPFE proliferating dramatically on the second CT, again highlighted on image overlays of PPFE regions (bottom row).

PPFE progression above scan noise

89 out of 414 (21%) patients in the IPF cohort and 25 out of 98 (26%) patients in the FHP cohort had progressive radiological PPFE as determined by Δ-PPFE >1.25%/year (figure 3). Demographic data, baseline pulmonary function tests, and mean visual ILD extent and computerised PPFE scores for non-progressive PPFE patients without clinically important PPFE at baseline, non-progressive PPFE patients with clinically important PPFE at baseline, and progressive PPFE patients are shown in supplementary tables S15 and S16.

Definitive PPFE change above scan noise (Δ-PPFE-adj) was independently associated with mortality in multivariable Cox regression models in the IPF cohort (HR 1.25, 95% CI 1.16–1.34, p<0.0001) and the FHP cohort (HR 1.16, 95% CI 1.00–1.35, p=0.045) (table 2) regardless of the degree of ILD progression or the presence of clinically important PPFE at baseline. Results were maintained in non-imputed models and in models not adjusted for baseline presence of clinically important PPFE (supplementary tables S17 and S18). Sensitivity analyses investigating noise threshold values in the range 0.5%/year to 1.5%/year showed maintained results (supplementary table S19). Kaplan–Meier analyses reflected the poor survival in patients with progressive PPFE (figure 4).

TABLE 2 Association of Δ-PPFE-adj with mortality in multivariable Cox regression models in the IPF cohort and in the FHP cohort

Variable	Hazard ratio	95% confidence interval	p-value	Model C-index
IPF				
Baseline age years	1.00	0.99–1.02	0.73	0.75
Male sex	1.46	1.00–2.14	0.047	
Ever-smoker	1.22	0.87–1.71	0.25	
Baseline emphysema (absent/present)	0.93	0.67–1.31	0.69	
Antifibrotic treatment (never/ever)	0.72	0.54–0.97	0.033	
Δ-ILD %/year	1.01	0.98–1.03	0.62	
Baseline PPFE extent >2.5%	1.72	1.27–2.33	0.0006	
Baseline D_{LCO} % predicted	0.96	0.94–0.97	<0.0001	
Δ-PPFE-adj %/year	1.25	1.16–1.34	<0.0001	
FHP				
Baseline age years	1.08	1.03–1.13	0.004	0.79
Male sex	1.02	0.41–2.52	0.97	
Ever-smoker	1.75	0.63–4.86	0.27	
Baseline emphysema (absent/present)	0.71	0.29–1.74	0.44	
Δ-ILD %/year	1.13	1.04–1.23	0.004	
Baseline PPFE extent >2.5%	2.11	0.89–5.00	0.086	
Baseline D_{LCO} % predicted	0.96	0.93–0.99	0.014	
Δ-PPFE-adj %/year	1.16	1.00–1.35	0.045	

Models in all cohorts were adjusted for patient age, sex, smoking history (never/ever), emphysema presence at baseline, clinically important PPFE at baseline (baseline PPFE >2.5% upper-zone pleural surface area), baseline D_{LCO} % predicted, annualised change in interstitial lung disease extent (Δ-ILD) and Δ-PPFE-adj. Models in the IPF cohort were also adjusted for antifibrotic treatment (never/ever). Δ-PPFE-adj: annualised change in computerised upper-zone PPFE between scans above scan noise; IPF: idiopathic pulmonary fibrosis; FHP: fibrotic hypersensitivity pneumonitis; PPFE: pleuroparenchymal fibroelastosis; D_{LCO}: diffusing capacity of the lung for carbon monoxide.

Discussion

In our study of computerised quantitation of radiological PPFE change we demonstrate that in patients with IPF and FHP, worsening computerised PPFE independently associates with increased patient mortality with similar effect sizes seen in two separate patient populations. Limited associations were seen between PPFE worsening and measures used to estimate disease progression in IPF and FHP (radiological ILD progression and FVC decline) suggesting that PPFE progression occurs independently of established fibrotic pathways. When evaluating morphologically important PPFE change, over 20% of patients in the IPF and FHP cohorts demonstrated progressive PPFE.

Radiological PPFE on CT has been well characterised over the last 10 years following detailed histopathological–radiological correlative studies [24–26]. PPFE quantification has primarily been attempted using crude categorical visual scales of CT disease extent [11, 14], but computer quantitation can improve identification of PPFE patients with a poor prognosis [11]. In the current study the high prevalence of PPFE noted in FHP [15] and similar survival between FHP and IPF patients [27, 28] underpinned the rationale for extending our analysis to a multicentred FHP cohort. We show that across two cohorts of patients with fibrosing lung disease, similar proportions of patients demonstrated a progressive PPFE phenotype. The disassociation between PPFE progression and ILD progression in the current study (as delineated by CT change in visual ILD scores or FVC decline) matched disassociation between baseline PPFE extent and measures of IPF severity in our previous study [11].

While PPFE has been increasingly reported in patients with underlying lung fibrosis [11, 14], PPFE has also been identified in the setting of bone marrow [25, 29] and lung transplantation [30–32] recipients, patients exposed to dusts [33] and as a long-term sequela of patients receiving chemotherapeutic agents [34]. Hypotheses for potential causes of PPFE might include occult infectious agents, excessive reaction to recurrent pulmonary infections in patients with pre-existing immune dysregulation or a manifestation of a pulmonary malignancy. Associations seen in patients with PPFE include genetic predispositions (telomere-related gene mutations [35, 36]), recurrent pulmonary infections [24] and ischaemia in apical lung vessels [30, 37, 38]. Despite the high prevalence of PPFE reported in patients with interstitial fibrosis,

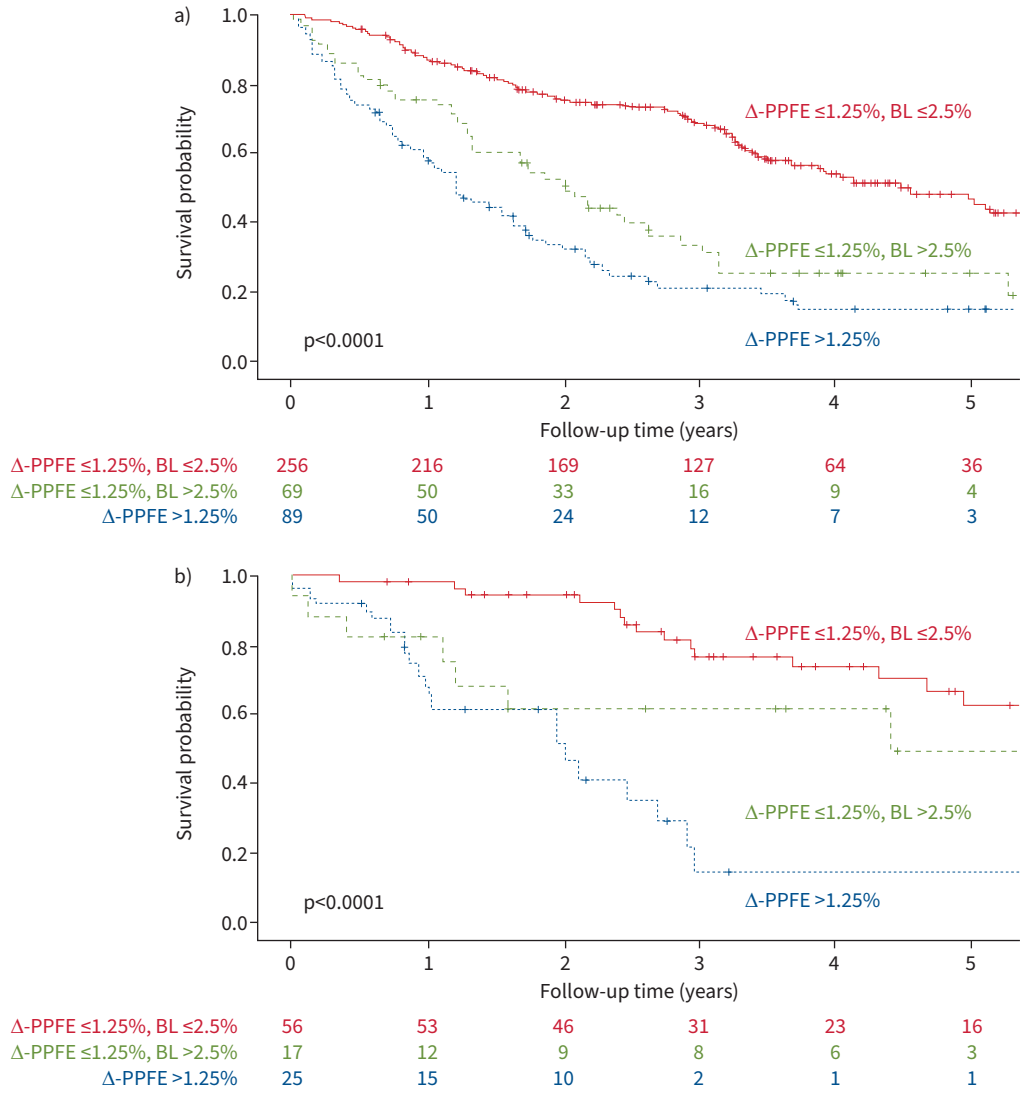

FIGURE 4 The impact of progressive PPFE and clinically important PPFE at baseline on survival in IPF and FHP patients. Kaplan–Meier survival curves for: 1) patients without clinically important PPFE at baseline and without progressive PPFE ("Δ-PPFE ⩽1.25%, BL ⩽2.5%"); 2) patients with clinically important PPFE at baseline and without progressive PPFE ("Δ-PPFE ⩽1.25%, BL >2.5%"); and 3) patients with progressive PPFE ("Δ-PPFE >1.25%") in a) the IPF cohort and b) the FHP cohort. Progressive PPFE was defined as patients with Δ-PPFE >1.25%/year change in pleural surface area. Clinically important PPFE at baseline was defined as PPFE baseline extent >2.5%. Survival curves were truncated at 5 years. Data below each plot show number of patients at risk at 1-year intervals. p-values are based on a log-rank test of differences in the survival curves of each plot. IPF: idiopathic pulmonary fibrosis; FHP: fibrotic hypersensitivity pneumonitis; PPFE: pleuroparenchymal fibroelastosis; Δ-PPFE: annualised change in computerised upper-zone PPFE between scans; BL: baseline.

the location of PPFE in the lung apices, its occurrence in patients without fibrosis and specifically the lack of major association between PPFE progression and measures of fibrosis progression support our contention [11] that PPFE occurring in fibrosing lung diseases represents a distinct disease endotype.

The increased mortality seen in patients with progressive PPFE may reflect the replacement of upper-zone lung tissue in patients with IPF/FHP with an elastotic process. The lung in the upper zones is often spared in IPF, and its loss may disproportionately impact gas exchange in patients where the middle/lower zones demonstrate airspace and vascular destruction. It has also been observed in studies using corrosion casting of the lung microvasculature that extensive intussusceptive angiogenesis occurs in areas of PPFE [39]. It is

therefore possible that as PPFE proliferates, there may be accentuation in ventilation–perfusion mismatches which in turn further exacerbate hypoxia in patients with concomitant fibrosing lung disease.

There remains an urgent need to invest more resources to examine specific treatments that can target PPFE in the subgroups of patients with IPF and FHP. Application of computer tools to baseline CT data [11] can aid in cohort enrichment when recruiting patients to therapeutic trials for PPFE, which can in turn improve the power of clinical trials. Therapeutic trials in IPF have been constrained by a lack of reliable end-points, which necessitate larger sample sizes and therefore more expensive trials. Our current study emphasises the potential for computer-based delineation of PPFE progression to act as a drug trial end-point when determining treatment response.

There were several limitations to the current study. Reasons for performing longitudinal imaging in IPF and FHP patients can be varied. Disproportionately, imaging is repeated following clinical deterioration. Consequently, patients with acute exacerbations, infections, pneumothoraces [25, 40] and pneumomediastinum, which occur with increased frequency in PPFE, were not infrequent in our study cohorts (figure 1, supplementary figure S1). These patients and those with coexisting lung malignancies were excluded from the current analysis to avoid non-PPFE pathology being mistakenly characterised as PPFE by the computer. We may therefore have underestimated the prevalence of progressive PPFE occurring in IPF and FHP. In addition, we did not have detailed information in the study population on the use of immunomodulatory therapies, which could have influenced the progression of PPFE.

Through a retrospective analysis of non-protocolised scans, our study demonstrated a strong mortality signal in real-world multicentred noisy data. While we adjusted our analyses to account for biases between study centres through mixed-effects models and frailty Cox models, we also tried to delineate measurement noise associated with quantitative analysis of longitudinal CT imaging. As it is only necessary to detect a digital signature equivalent to PPFE on one single voxel out of the many millions of lung voxels present on a single CT, some measure of PPFE will invariably be detected by computational CT analysis. However not all PPFE or PPFE change detected by a computer is real, *e.g.*, PPFE change could be artificially inflated by a poor inspiratory effort on a second timepoint CT. We estimated the degree of noise from longitudinal CT analysis of PPFE change as 50% of the standard deviation of PPFE seen at baseline, in accordance with similar prior work in IPF. The similar effect size of our adjusted PPFE quantitation on mortality analysis across the two study cohorts reinforces our belief that our estimation of noise is appropriate and has clinical utility.

In conclusion, our study highlights the independent deleterious prognostic effect of worsening computerised PPFE-like lesions in patients with IPF and FHP. PPFE progression only associated weakly with measures of ILD progression in IPF suggesting that the distinct disease trajectories for ILD and PPFE may represent separate pathophysiological pathways. Over 20% of patients in the two study cohorts were identified with a progressive PPFE phenotype which independently associated with mortality. Given the need for new targeted therapies for PPFE, our computer-based quantitation of PPFE could act as a new end-point in randomised clinical trials.

Provenance: Submitted article, peer reviewed.

Acknowledgements: The authors would like to thank the family of Nathalie Soffe for their support of research into improving the understanding of PPFE development.

Author contributions: E. Gudmundsson, A. Zhao, I. Stewart, A.U. Wells, S.M. Janes, D.C. Alexander and J. Jacob contributed to study design and data interpretation. E. Gudmundsson, A. Zhao, N. Mogulkoc, M.G. Jones, C.H.M. van Moorsel, W. Wuyts, J. Porter, S. Verleden, R. Savas, C.J. Brereton, H.W. van Es, T. Goos, M. Heightman, O. Unat, K. Pontoppidan, F. van Beek, M. Veltkamp, T. Wallis, B. Gholipour, L. De Sadeleer, E. Denneny, A. Nair, R. Chapman, M. Vermant, A. Ahmed, M. Taylor, M. Duncan, A. Procter, H. Garthwaite and J. Jacob were responsible for data acquisition. E. Gudmundsson, A. Zhao, I. Stewart and J. Jacob contributed to the statistical analysis. E. Gudmundsson and J. Jacob prepared the first draft of the manuscript. E. Gudmundsson and J. Jacob were responsible for study data integrity. All authors reviewed the manuscript and approved the final submitted version.

Conflict of interest: J. Jacob reports fees from Boehringer Ingelheim, Roche, NHSX, Takeda and GlaxoSmithKline unrelated to the submitted work. J. Jacob was supported by Wellcome Trust Clinical Research Career Development Fellowship 209553/Z/17/Z and the NIHR Biomedical Research Centre at University College London. S.M. Janes reports fees from AstraZeneca, Bard1 Bioscience, Achilles Therapeutics and Janssen unrelated to the submitted work. S.M. Janes received assistance for travel to meetings from AstraZeneca to American Thoracic

Conference 2018 and from Takeda to World Conference Lung Cancer 2019, and is the Investigator Lead on grants from GRAIL Inc, GlaxoSmithKline plc and Owlstone. A.U. Wells reports personal fees and nonfinancial support from Boehringer Ingelheim, Bayer and Roche Pharmaceuticals; and personal fees from Blade, outside of the submitted work. The remaining authors have nothing to disclose.

Support statement: This research was funded in whole or in part by the Wellcome Trust (209553/Z/17/Z). This project, J. Jacob, E. Gudmundsson, E. Denneny, J. Porter and S.M. Janes were also supported by the NIHR UCLH Biomedical Research Centre, UK. M.G. Jones, T. Wallis and C.J. Brereton acknowledge the support of the NIHR Southampton Biomedical Research Centre. Funding information for this article has been deposited with the Crossref Funder Registry.

References

1 Hansell DM, Bankier AA, MacMahon H, *et al.* Fleischner Society: glossary of terms for thoracic imaging. *Radiology* 2008; 246: 697–722.
2 Raghu G, Remy-Jardin M, Myers JL, *et al.* Diagnosis of idiopathic pulmonary fibrosis. An Official ATS/ERS/JRS/ALAT Clinical practice guideline. *Am J Respir Crit Care Med* 2018; 198: e44–e68.
3 Ley B, Collard HR, King TE. Clinical course and prediction of survival in idiopathic pulmonary fibrosis. *Am J Respir Crit Care Med* 2011; 183: 431–440.
4 Jacob J, Aksman L, Mogulkoc N, *et al.* Serial CT analysis in idiopathic pulmonary fibrosis: comparison of visual features that determine patient outcome. *Thorax* 2020; 75: 648–654.
5 Balestro E, Cocconcelli E, Giraudo C, *et al.* High-resolution CT change over time in patients with idiopathic pulmonary fibrosis on antifibrotic treatment. *J Clin Med* 2019; 8: 1469.
6 Park HJ, Lee SM, Song JW, *et al.* Texture-based automated quantitative assessment of regional patterns on initial CT in patients with idiopathic pulmonary fibrosis: relationship to decline in forced vital capacity. *AJR Am J Roentgenol* 2016; 207: 976–983.
7 Taha N, D'Amato D, Hosein K, *et al.* Longitudinal functional changes with clinically significant radiographic progression in idiopathic pulmonary fibrosis: are we following the right parameters? *Respir Res* 2020; 21: 119.
8 Jacob J, Bartholmai BJ, Rajagopalan S, *et al.* Mortality prediction in idiopathic pulmonary fibrosis: evaluation of computer-based CT analysis with conventional severity measures. *Eur Respir J* 2017; 49: 1601011.
9 Jacob J, Bartholmai BJ, Rajagopalan S, *et al.* Predicting outcomes in idiopathic pulmonary fibrosis using automated computed tomographic analysis. *Am J Respir Crit Care Med* 2018; 198: 767–776.
10 Jacob J, Bartholmai BJ, van Moorsel CHM, *et al.* Longitudinal prediction of outcome in idiopathic pulmonary fibrosis using automated CT analysis. *Eur Respir J* 2019; 54: 1802341.
11 Gudmundsson E, Zhao A, Mogulkoc N, *et al.* Pleuroparenchymal fibroelastosis in idiopathic pulmonary fibrosis: survival analysis using visual and computer-based computed tomography assessment. *EClinicalMedicine* 2021; 38: 101009.
12 Watanabe K. Pleuroparenchymal fibroelastosis: its clinical characteristics. *Curr Respir Med Rev* 2014; 9: 229–237.
13 Fujisawa T, Horiike Y, Egashira R, *et al.* Radiological pleuroparenchymal fibroelastosis-like lesion in idiopathic interstitial pneumonias. *Respir Res* 2021; 22: 290.
14 Bonifazi M, Sverzellati N, Negri E, *et al.* Pleuroparenchymal fibroelastosis in systemic sclerosis: prevalence and prognostic impact. *Eur Respir J* 2020; 56: 1902135.
15 Jacob J, Odink A, Brun AL, *et al.* Functional associations of pleuroparenchymal fibroelastosis and emphysema with hypersensitivity pneumonitis. *Respir Med* 2018; 138: 95–101.
16 Nasser M, Si-Mohamed S, Turquier S, *et al.* Nintedanib in idiopathic and secondary pleuroparenchymal fibroelastosis. *Orphanet J Rare Dis* 2021; 16: 419.
17 Flaherty KR, Wells AU, Cottin V, *et al.* Nintedanib in progressive fibrosing interstitial lung diseases. *N Engl J Med* 2019; 381: 1718–1727.
18 Norman GR, Sloan JA, Wyrwich KW. Interpretation of changes in health-related quality of life: the remarkable universality of half a standard deviation. *Med Care* 2003; 41: 582–592.
19 Swigris JJ, Wamboldt FS, Behr J, *et al.* The 6 min walk in idiopathic pulmonary fibrosis: longitudinal changes and minimum important difference. *Thorax* 2010; 65: 173–177.
20 Humphries SM, Swigris JJ, Brown KK, *et al.* Quantitative high-resolution computed tomography fibrosis score: performance characteristics in idiopathic pulmonary fibrosis. *Eur Respir J* 2018; 52: 1801384.
21 Koenker R. A note on studentizing a test for heteroscedasticity. *J Econom* 1981; 17: 107–112.
22 Harrell FE, Califf RM, Pryor DB, *et al.* Evaluating the yield of medical tests. *JAMA* 1982; 247: 2543–2546.
23 Nakagawa S, Schielzeth H. A general and simple method for obtaining R2 from generalized linear mixed-effects models. *Methods Ecol Evol* 2013; 4: 133–142.
24 Reddy TL, Tominaga M, Hansell DM, *et al.* Pleuroparenchymal fibroelastosis: a spectrum of histopathological and imaging phenotypes. *Eur Respir J* 2012; 40: 377–385.

25 von der Thüsen JH, Hansell DM, Tominaga M, *et al.* Pleuroparenchymal fibroelastosis in patients with pulmonary disease secondary to bone marrow transplantation. *Mod Pathol* 2011; 24: 1633–1639.
26 Kusagaya H, Nakamura Y, Kono M, *et al.* Idiopathic pleuroparenchymal fibroelastosis: consideration of a clinicopathological entity in a series of Japanese patients. *BMC Pulm Med* 2012; 12: 72.
27 Jacob J, Bartholmai BJ, Egashira R, *et al.* Chronic hypersensitivity pneumonitis: identification of key prognostic determinants using automated CT analysis. *BMC Pulm Med* 2017; 17: 81.
28 Salisbury ML, Gu T, Murray S, *et al.* Hypersensitivity pneumonitis: radiologic phenotypes are associated with distinct survival time and pulmonary function trajectory. *Chest* 2019; 155: 699–711.
29 Parish JM, Muhm JR, Leslie KO. Upper lobe pulmonary fibrosis associated with high-dose chemotherapy containing BCNU for bone marrow transplantation. *Mayo Clin Proc* 2003; 78: 630–634.
30 Pakhale SS, Hadjiliadis D, Howell DN, *et al.* Upper lobe fibrosis: a novel manifestation of chronic allograft dysfunction in lung transplantation. *J Heart Lung Transplant* 2005; 24: 1260–1268.
31 Konen E, Weisbrod GL, Pakhale S, *et al.* Fibrosis of the upper lobes: a newly identified late-onset complication after lung transplantation? *AJR Am J Roentgenol* 2003; 181: 1539–1543.
32 Mariani F, Gatti B, Rocca A, *et al.* Pleuroparenchymal fibroelastosis: the prevalence of secondary forms in hematopoietic stem cell and lung transplantation recipients. *Diagn Interv Radiol* 2016; 22: 400–406.
33 Xu L, Rassaei N, Caruso C. Pleuroparenchymal fibroelastosis with long history of asbestos and silicon exposure. *Int J Surg Pathol* 2018; 26: 190–193.
34 Beynat-Mouterde C, Beltramo G, Lezmi G, *et al.* Pleuroparenchymal fibroelastosis as a late complication of chemotherapy agents. *Eur Respir J* 2014; 44: 523–527.
35 Newton CA, Batra K, Torrealba J, *et al.* Telomere-related lung fibrosis is diagnostically heterogeneous but uniformly progressive. *Eur Respir J* 2016; 48: 1710–1720.
36 Nunes H, Jeny F, Bouvry D, *et al.* Pleuroparenchymal fibroelastosis associated with telomerase reverse transcriptase mutations. *Eur Respir J* 2017; 49: 1602022.
37 Thusen J. Pleuroparenchymal fibroelastosis: its pathological characteristics. *Curr Respir Med Rev* 2014; 9: 238–247.
38 van der Oord K, Rietema H, von der Thusen JH, *et al.* Pleuroparenchymal fibroelastosis with prominent thrombosis. *Pathol Int* 2017; 67: 56–58.
39 Ackermann M, Stark H, Neubert L, *et al.* Morphomolecular motifs of pulmonary neoangiogenesis in interstitial lung diseases. *Eur Respir J* 2020; 55: 1900933.
40 Sverzellati N, Zompatori M, Poletti V, *et al.* Small chronic pneumothoraces and pulmonary parenchymal abnormalities after bone marrow transplantation. *J Thorac Imaging* 2007; 22: 230–234.